Journal of Global Optimization **16:** 325–341, 2000.

Approximate energy minimization for large Lennard-Jones clusters

YUEFAN DENG[1,2] and CARLOS RIVERA[2]
[1]*IBM Thomas J. Watson Research Center, Yorktown Heights, NY 10598, USA;* [2]*Department of Applied Mathematics, State University of New York, Stony Brook, NY 11794-3600, USA*

(Received: 20 October 1997; accepted in revised form: 5 October 1999)

Abstract. We have designed a simple method to place particles on lattices, concentric shells and icosahedral concentric layers for minimizing the total energy of Lennard-Jones clusters, approximately, by analytical means. The most significant difference of our schemes from others is the dramatic reduction of parameters, which allows the study of large clusters, not possible otherwise. We present the derivation of formulae for minimal per-particle energy and for inter-particle distance. We also present their asymptotic values for large number of particles.

Key words: Global optimization, Lennard-Jones clusters, Asymptotic convergence

1. Introduction

Many people [1–10] have been working on the numerical minimization of the energy of systems consisting of particles interacting under the Lennard-Jones potential,

$$U(a) = \frac{1}{a^{12}} - \frac{2}{a^6},$$

of the so-called Lennard-Jones clusters. We have designed a simple method which renders the energy as a single parameter and makes the energy trivial to minimize. The results not only give an asymptotic understanding of the system but also provides excellent initialization for CPU-intense numerical minimization.

We illustrate the methods by doing the calculation on lattices in one, two and three dimensions, as well as on spheres in two and three dimensions and on icosahedra in three dimensions. We also compare our results with those obtained by a different method [11].

2. Derivation of interactions

We employ a similar procedure to all cases. First, express the position of each particle with appropriate coordinates, then, find the distance between two arbitrary particles, and finally, obtain the total energy of the system.

2.1. FOR PARTICLES ON LATTICES

In one dimension: We indicate the position of an arbitrary particle by $a_i = ia$ where a is the distance between two consecutive particles and i ranges from 1 to N, N being the total number of particles. The distance between a pair $(i,\ j)$ is $a_{ij} = (i - j)a$ and the total energy of N particles is then

$$E(a) = \frac{1}{2}\left(\frac{1}{a^{12}}\sum_{i\neq j=1}^{N}\frac{1}{(i-j)^{12}} - \frac{1}{a^6}\sum_{i\neq j=1}^{N}\frac{2}{(i-j)^6}\right).$$

Define two functions $F(N)$ and $G(N)$

$$F(N) = \sum_{i\neq j=1}^{N}\frac{1}{(i-j)^{12}},$$

$$G(N) = \sum_{i\neq j=1}^{N}\frac{1}{(i-j)^6}.$$

E can now be written as

$$E(a) = \frac{1}{2}\left(\frac{1}{a^{12}}\,F(N) - \frac{2}{a^6}\,G(N)\right). \tag{1}$$

This expression is general for all of six cases we discuss: 1D, 2D and 3D lattices, 2D and 3D sphere, and 3D icosahedron. The specific form of $F(N)$ and $G(N)$ depends on the dimension and on the configuration of the problem. In fact, since the parameter a always factorizes out in the expression for the distance, we can generalize Equation (1). For any pair-wise potential of the form

$$U(a) = R(a) - A(a), \tag{2}$$

the corresponding total energy form is

$$E(a) = \frac{1}{2}\,(R(a)F(N) - A(a)G(N)) \tag{3}$$

Therefore, the problem lies in finding the analytical forms for $F(N)$ and $G(N)$. These functions are very complicated summations whose indexes are implicit functions of N and of previous indexes. It is however simple to use a computer to evaluate $F(N)$ and $G(N)$. That is how we obtained our test numerical results. These results were then fitted into the curves that were numerically reasonable rather than physically significant.

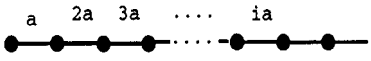

Figure 1. One dimensional lattice. The only parameter is a, the inter-particle distance.

For Lennard-Jones clusters, a_0, the value of parameter a at which E is minimal is

$$a_0 = \left(\frac{F(N)}{G(N)}\right)^{1/6}, \tag{4}$$

and the associated minimal energy per particle is

$$\varepsilon = -\frac{1}{2}\,\frac{G^2(N)}{NF(N)}. \tag{5}$$

In two dimensions: Take two points of our lattice each labeled by two coordinates so that we have $a_{\alpha\beta} = (\alpha a,\ \beta a)$ and $a_{\gamma\rho} = (\gamma a,\ \beta a)$, the distance between the two is then

$$a_{\alpha\beta\gamma\rho} = \sqrt{(\alpha a - \gamma a)^2 + (\beta a - \rho a)^2}$$

a is factorized out, leaving

$$a_{\alpha\beta\gamma\rho} = a\sqrt{\alpha^2 + \gamma^2 + \beta^2 + \rho^2 - 2\alpha\gamma - 2\beta\rho}$$

We define $F(N)$ and $G(N)$ as before:

$$F(N) = \sum_{\alpha,\beta,\gamma,\rho=0}^{I} (\alpha^2 + \gamma^2 + \beta^2 + \rho^2 - 2\alpha\gamma - 2\beta\rho)^{-6}$$

where $I = \sqrt{N} - 1$ and $\alpha \neq \gamma$ if $\beta = \rho$ and $\beta \neq \rho$ if $\alpha = \gamma$

$$G(N) = \sum_{\alpha,\beta,\gamma,\rho=0}^{I} (\alpha^2 + \gamma^2 + \beta^2 + \rho^2 - 2\alpha\gamma - 2\beta\rho)^{-3}$$

where $I = \sqrt{N} - 1$ and $\alpha \neq \gamma$ if $\beta = \rho$ and $\beta \neq \rho$ if $\alpha = \gamma$.

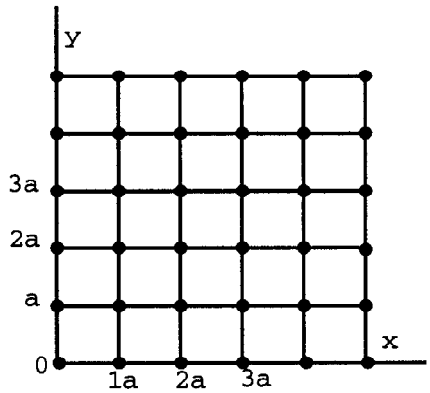

Figure 2. Two dimensional lattice. The only parameter is a, the inter-particle distance along the two axes.

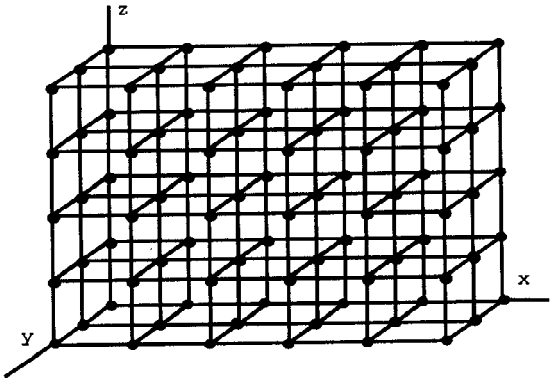

Figure 3. Three dimensional lattice. The only parameter is a.

In three dimensions: Each of the functions $F(N)$ and $G(N)$ consists of six sums for the three dimensional case. Take two points $a_{\alpha\beta\gamma} = (\alpha a,\ \beta a,\ \gamma a)$ and $a_{\sigma\rho\delta} = (\sigma a,\ \rho a,\ \delta a)$ their distance is

$$a_{\alpha\beta\gamma\sigma\rho\delta} = \sqrt{(\alpha a - \sigma a)^2 + (\beta a - \rho a)^2 + (\gamma a - \delta a)^2}$$

a is factorized out leaving

$$a_{\alpha\beta\gamma\sigma\rho\delta} = a\sqrt{\alpha^2 + \sigma^2 + \beta^2 + \rho^2 + \gamma^2 + \delta^2 - 2\alpha\sigma - 2\beta\sigma - 2\beta\rho - 2\gamma\delta}$$

$F(N)$ and $G(N)$ are now:

$$F(N) = \sum_{\alpha,\beta,\gamma,\sigma,\rho,\delta=0}^{I} (\alpha^2 + \sigma^2 + \beta^2 + \rho^2 + \gamma^2 + \delta^2 - 2\alpha\sigma - 2\beta\rho - 2\gamma\delta)^{-6}$$

$$G(N) = \sum_{\alpha,\beta,\gamma,\sigma,\rho,\delta=0}^{I} (\alpha^2 + \sigma^2 + \beta^2 + \rho^2 + \gamma^2 + \delta^2 - 2\alpha\sigma - 2\beta\rho - 2\gamma\delta)^{-3}$$

where $I = \sqrt[3]{N} - 1$ and any two equal points are excluded from summation.

2.2. FOR PARTICLES ON SHELLS OF A SPHERE

In two dimensions: The particles are distributed along concentric rings. The radius of the i-th ring, counted outward from the center, is ia and the distance along the arc between two neighboring particles in one particular ring is equivalent for all particles, and on all rings, and it is $(\pi/3)a$. This way, the number of particles in ring i is $6i$. The position of any particle is defined by its ring number i and its location along the arc-length of its ring starting from an arbitrary north pole which is the same for all rings. The range of this last parameter is a function of the first.

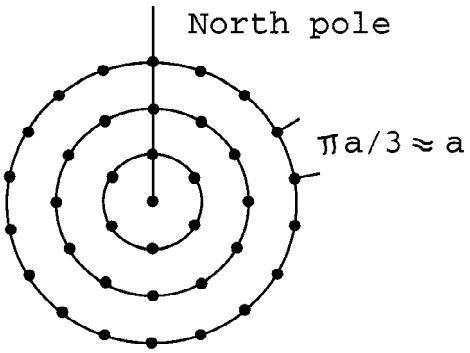

Figure 4. Particles on concentric rings. The parameter is a, the radial distance between two consecutive rings and the approximate nearest neighbor distance for any particle.

Obviously, we can vary the distances between the successive rings and rotate each ring by a certain amount for better minimization at added complexity.

In polar coordinates we have

$$a_{i\alpha} = \left(ia,\ \frac{\alpha\pi}{3i}\right)$$

where $\alpha = 0 \ldots 6i - 1$.

Given two points $a_{i\alpha}$ and $a_{j\beta}$, the distance between them is

$$a_{i\alpha j\beta} = a\sqrt{i^2 + j^2 - 2ij\cos\left(\frac{\pi}{3}\left(\frac{\alpha}{i} - \frac{\beta}{j}\right)\right)}$$

Write $f_{i\alpha j\beta} = a_{i\alpha j\beta}/a$, then $F(N)$ and $G(N)$ can be written as

$$F(N) = \sum_{i=1}^{I}\sum_{\alpha=0}^{6i-1}\sum_{j=1}^{I}\sum_{\beta=0}^{6j-1}\frac{1}{f_{i\alpha j\beta}^{12}}$$

$$G(N) = \sum_{i=1}^{I}\sum_{\alpha=0}^{6i-1}\sum_{j=1}^{I}\sum_{\beta=0}^{6j-1}\frac{1}{f_{i\alpha j\beta}^{6}}$$

where I is defined implicitly by $6(\sum_{k=1}^{I} k) + N$. Note the fact that we need to fill all rings imposes a constraint on what values of N can be used to evaluate ε.

In order to include the one necessary particle at the center, we must make a small modification to $F(N)$ and $G(N)$ to obtain the complete result,

$$F(N) = \sum_{i=1}^{I}\sum_{\alpha=0}^{6i-1}\sum_{j=1}^{I}\sum_{\beta=0}^{6j-1}\frac{1}{f_{i\alpha j\beta}^{12}} + 2\sum_{i=1}^{I}\sum_{\alpha=0}^{6i-1}\frac{1}{i^{12}}$$

$$G(N) = \sum_{i=1}^{I}\sum_{\alpha=0}^{6i-1}\sum_{j=1}^{I}\sum_{\beta=0}^{6j-1}\frac{1}{f_{i\alpha j\beta}^{6}} + 2\sum_{i=1}^{I}\sum_{\alpha=0}^{6i-1}\frac{1}{i^{6}}$$

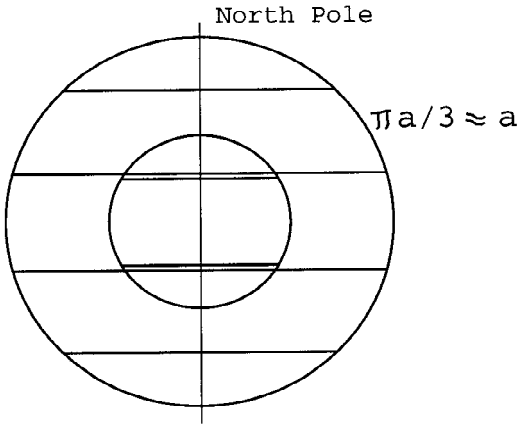

Figure 5. Cross section of the sphere. The lines represent planes that cut the sphere in rings. Using the method of the 2D spheres (i.e. rings), particles are then distributed in the rings. In this picture there are two shells.

In three dimensions: Fixing a north pole the shells are then cut into rings perpendicular to this south-north line. The spacing of the rings, as measured along the arc of a geodesic that goes through both south and north poles, is fixed and equals $(\pi/3)a$, where a is the radius of the smallest shell. The number of these rings depends on the radius of the shell, for a shell of radius ia there are $3i + 1$ rings (including the top and bottom rings which shrink to a dot and thus include one particular each). Each of these rings is then treated as in the previous 2D case, introducing a new parameter α which indicates which ring we are treating starting from north pole where $\alpha = 0$ and going down to the south pole where $\alpha = 3i$, for shell i.

If we wanted the separation between adjacent particles along the ring to be exactly a, then the number of particles in the i-th ring would be $2\pi ia|\sin(\frac{\pi\alpha}{3i})|$. Obviously, we have to round the whole expression to obtain an integer for the number of particles. The distance along the arc between adjacent particles in the i-th ring then becomes

$$\frac{2\pi ia\left|\sin\left(\frac{\pi\alpha}{3i}\right)\right|}{\left[6i\sin\left(\frac{\pi\alpha}{3i}\right)\right]}$$

where [ ] is the usual operator for rounding to the nearest integer and taking absolute value. A particle is then localized completely by its shell number i, its ring number α and its position on the ring that we label β. In spherical coordinates we have

$$\alpha_{i\alpha\beta} = \left(ia,\ \frac{\alpha\pi}{3i},\ \frac{2\pi\beta}{\left[6i\sin\left(\frac{\pi\alpha}{3i}\right)\right]}\right)$$

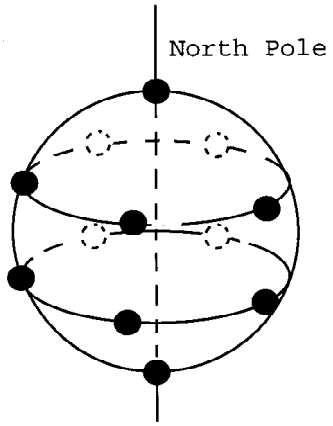

Figure 6. 3D perspective of the first shell.

where the parameters range as follows

$$\begin{aligned} i &= 1 \ldots I \\ \alpha &= 0 \ldots 3i \\ \beta &= 0 \ldots \left[6i \sin\left(\frac{\pi\alpha}{3i}\right)\right] - 1 \end{aligned}$$

and where I is an implicit function of N. We did not obtain the analytical expression but simply computed N numerically. To simplify things we denote the coordinates of a particle as $a_{i\alpha\beta} = (ia,\ \theta_{i\alpha},\ \phi_{i\alpha\beta})$. The distance between two particle $a_{i\alpha\beta}$ and $a_{j\gamma\sigma}$ is

$$\begin{aligned} a_{i\alpha\beta j\gamma\sigma} = ((&ia \sin\theta_{i\alpha} \cos\phi_{i\alpha\beta} - ja \sin\theta_{j\gamma} \cos\phi_{j\gamma\sigma})^2 + (ia \sin\theta_{i\alpha} \sin\phi_{i\alpha\beta} \\ &- ja \sin\theta_{j\gamma} \sin\phi_{j\gamma\sigma})^2 + (ia \cos\theta_{i\alpha} - ja \cos\theta_{j\gamma})^2)^{1/2} \end{aligned}$$

which simplifies to

$$a_{i\alpha\beta j\gamma\sigma} = a\sqrt{i^2 + j^2 - 2ij[\sin\theta_{i\alpha} \sin\theta_{j\gamma} \cos(\phi_{i,\alpha\beta} - \phi_{j,\gamma\sigma}) + \cos\theta_{i\alpha} \cos_{j\gamma}]}$$

Define $f_{i\alpha\beta j\gamma\sigma} = a_{i\alpha\beta j\gamma\sigma}/a$ and we obtain for $F(N)$ and $G(N)$ the following

$$\begin{aligned} F(N) &= \sum_{i,j=1}^{I} \sum_{\alpha,\gamma=0}^{\alpha=3i,\gamma=3j} \sum_{\beta,\rho=0}^{\beta_{\max}\rho_{\max}} \frac{1}{f_{i\alpha\beta j\gamma\sigma}^{12}} \\ G(N) &= \sum_{i,j=1}^{I} \sum_{\alpha,\gamma=0}^{\alpha=3i,\gamma=3j} \sum_{\beta,\rho=0}^{\beta_{\max}\rho_{\max}} \frac{1}{f_{i\alpha\beta j\gamma\sigma}^{6}} \end{aligned}$$

Where $\beta_{\max}$ and $\rho_{\max}$ refer to the limits mentioned above. Adding the particle at the center of the structure we revise $F(N)$ and $G(N)$,

$$F(N) = \sum_{i,j=1}^{I} \sum_{\alpha,\gamma=0}^{\alpha=3i,\gamma=3j} \sum_{\beta,\rho=0}^{\beta_{\max}\rho_{\max}} \frac{1}{f_{i\alpha\beta j\gamma\sigma}^{12}} + 2\sum_{i=1}^{I}\sum_{\alpha=0}^{3i}\sum_{\beta=0}^{\beta_{\max}} \frac{1}{i^{12}}$$

$$G(N) = \sum_{i,j=1}^{I} \sum_{\alpha,\gamma=0}^{\alpha=3i,\gamma=3j} \sum_{\beta,\rho=0}^{\beta_{\max}\rho_{\max}} \frac{1}{f_{i\alpha\beta j\gamma\sigma}^{6}} + 2\sum_{i=1}^{I}\sum_{\alpha=0}^{3i}\sum_{\beta=0}^{\beta_{\max}} \frac{1}{i^{6}}$$

2.3. FOR PARTICLES ON ICOSAHEDRAL SHAPED SHELLS

In three dimensions: We have also tried a configuration consisting of concentric layers of icosahedral shape. An algorithm was developed to distribute particles on the surface of each of the twenty triangular faces of each layer. As previously done, a parameter a was defined and factored out of the expression for the distance between two given particles rendering the minimization of the energy trivial to compute. In our construction a was the length of the side of the smallest icosahedron.

The way particles were distributed in each triangular face is shown in Figure 7. Each face of the n-th layer contained n concentric triangles and one particle at the center. The distance between any two consecutive particles on the same triangle is a. The length of any side of any triangle is always a multiple of a. In this way, particles are distributed uniformly on each layer.

The algorithm for this configuration was much more complicated than for the previous cases, however it did not improve the results obtained before by the simple lattice scheme.

The convergent values for ε and a_0 in the icosahedron case are -4.722 and 1.674 respectively. While the corresponding ε and a_0 for the cubic lattices are -5.271 and

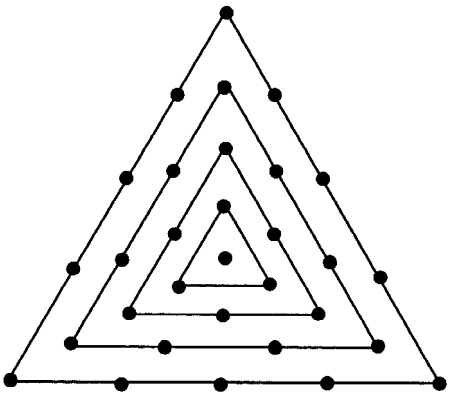

Figure 7. Distribution of particles on one of the 20 triangular faces of fourth icosahedral layer. The distance between every two particles along one side of any given triangle is a.

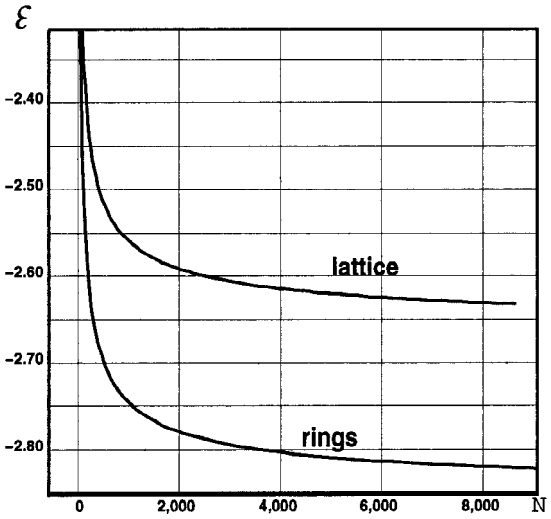

Figure 8. ε versus N for 2D lattice and rings. As shown in this figure, the minimal energy obtained by the spherical scheme is much lower than that obtained by the lattice scheme.

0.953, and -6.225 and 0.889 for the shells. Obviously, ε for the icosahedron is the highest. For two particles $a = 1$ minimizes the total energy. For large N, in the case of shells we found $a = 0.889$.

However, in the case of the icosahedron all particles have to take different values as the distances to their nearest neighbors because of the nature of icosahedron and our filling schemes, resulting in difficulty for an orchestrated action to minimize the total energy. We have, therefore, chosen not to include the details of these results for this configuration.

3. Numerical results

We have performed calculations on five of the six cases discussed in Section 2: 2D and 3D lattices, 2D and 3D spheres, and 3D icosahedron (neglecting the simple 1D lattice case). In each of these cases we have results for systems with as many as 50,000 particles. These results are shown in Tables 1, 2 and 3. The figures 8 to 20 depicts these results in graphical details for comparison and further analysis.

Table I. Results ε and a_0 for the 2D lattice.

N	ε	a_0	N	ε	a_0	N	ε	a_0
4	−1.120155	0.991232	1089	−2.563724	0.978266	4096	−2.615208	0.97789
9	−1.587178	0.986447	1156	−2.566839	0.978243	4225	−2.616055	0.977882
16	−1.839321	0.984123	1225	−2.569777	0.978221	4489	−2.617672	0.977871
25	−1.996584	0.982754	1296	−2.572553	0.978201	4356	−2.616876	0.977876
36	−2.103915	0.981854	1369	−2.575181	0.978181	4624	−2.618445	0.977865
49	−2.181798	0.981216	1444	−2.577571	0.978163	4761	−2.619196	0.977860
64	−2.240876	0.980741	1521	−2.580034	0.978146	4900	−2.619925	0.977854
81	−2.287221	0.980373	1600	−2.582280	0.978129	5041	−2.620634	0.977849
100	−2.324545	0.980080	1681	−2.584417	0.978114	5184	−2.621324	0.977844
121	−2.355248	0.979841	1764	−2.586452	0.978099	5329	−2.621994	0.977839
144	−2.380947	0.979642	1849	−2.588394	0.978084	5476	−2.622647	0.977834
169	−2.402772	0.979475	1936	−2.590248	0.978071	5625	−2.623282	0.977830
196	−2.421538	0.979331	2116	−2.593715	0.978045	5776	−2.623900	0.977825
225	−2.437846	0.979207	2209	−2.595339	0.978034	5929	−2.624503	0.977821
256	−2.452149	0.979099	2304	−2.596895	0.978022	6084	−2.625090	0.977817
289	−2.464795	0.979003	2401	−2.598388	0.978011	6241	−2.625662	0.977813
324	−2.476056	0.978918	2500	−2.599822	0.978001	6400	−2.626220	0.977809
400	−2.495245	0.978774	2601	−2.601200	0.977991	6561	−2.626764	0.977805
441	−2.503485	0.978713	2704	−2.602525	0.977981	6724	−2.627295	0.977801
484	−2.510986	0.978657	2809	−2.603800	0.977972	6889	−2.627813	0.977797
529	−2.517841	0.978606	2916	−2.605028	0.977963	7056	−2.628319	0.977793
576	−2.524131	0.978559	3025	−2.606212	0.977954	7225	−2.628813	0.977790
625	−2.529924	0.978516	3136	−2.607354	0.977946	7396	−2.629296	0.977786
676	−2.535275	0.978476	3249	−2.608456	0.977938	7569	−2.629768	0.977783
729	−2.540233	0.978439	3364	−2.609520	0.97793	7744	−2.630229	0.977779
784	−2.544841	0.978405	3481	−2.610548	0.977923	7921	−2.630679	0.977776
841	−2.549134	0.978373	3600	−2.611542	0.977915	8100	−2.631120	0.977773
900	−2.553143	0.978344	3721	−2.612503	0.977908	8281	−2.631551	0.977770
961	−2.556895	0.978316	3844	−2.613434	0.977901	8464	−2.631972	0.977767
1024	−2.560415	0.978290	3969	−2.614335	0.977895	8649	−2.632385	0.977764

Table II. Results ε and a_0 for the 2D rings.

N	ε	a_0	N	ε	a_0	N	ε	a_0
7	−1.790695	0.996435	5167	−2.809833	0.937678	19927	−2.834073	0.937437
19	−2.049368	0.989537	5419	−2.811004	0.937665	20419	−2.834375	0.937435
37	−2.253259	0.956292	5677	−2.812120	0.937653	20917	−2.834670	0.937432
61	−2.382833	0.949874	5941	−2.813186	0.937641	21421	−2.834958	0.937430
91	−2.469165	0.946318	6487	−2.815177	0.937620	21931	−2.835239	0.937427
127	−2.529984	0.944138	6769	−2.816109	0.937610	22447	−2.835514	0.937425
169	−2.574853	0.942701	7057	−2.817002	0.937600	22969	−2.835782	0.937423
217	−2.609196	0.941699	7351	−2.817859	0.937591	23497	−2.836044	0.937420
271	−2.636270	0.940970	7651	−2.818681	0.937583	24031	−2.836300	0.937418
331	−2.658132	0.940422	7957	−2.819470	0.937575	24571	−2.836551	0.937416
397	−2.676139	0.939997	8269	−2.820230	0.937567	25117	−2.836795	0.937414
469	−2.691216	0.939661	8587	−2.820960	0.937560	25669	−2.837035	0.937412
547	−2.704020	0.939389	8911	−2.821664	0.937553	26227	−2.837269	0.937410
631	−2.715025	0.939167	9241	−2.822341	0.937546	26791	−2.837499	0.937408
721	−2.724581	0.938981	9577	−2.822995	0.937539	27361	−2.837723	0.937407
817	−2.732956	0.938825	9919	−2.823625	0.937533	27937	−2.837943	0.937405
919	−2.740355	0.938691	10267	−2.824234	0.937527	28519	−2.838159	0.937403
1141	−2.752832	0.938477	10621	−2.824822	0.937522	29107	−2.838370	0.937401
1261	−2.758139	0.938390	10981	−2.825390	0.937516	29701	−2.838576	0.937400
1387	−2.762943	0.938314	11347	−2.825940	0.937511	30301	−2.838779	0.937398
1519	−2.767312	0.938246	11719	−2.826471	0.937506	30907	−2.838977	0.937397
1657	−2.771301	0.938185	12097	−2.826986	0.937501	31519	−2.839172	0.937395
1801	−2.774959	0.938131	12481	−2.827485	0.937496	32137	−2.839363	0.937393
1951	−2.778324	0.938082	12871	−2.827968	0.937492	32761	−2.839550	0.937392
2107	−2.781431	0.938038	13267	−2.828437	0.937487	33391	−2.839733	0.937390
2269	−2.784308	0.937998	13669	−2.828891	0.937483	34027	−2.839913	0.937389
2437	−2.786979	0.937962	14077	−2.829332	0.937479	34669	−2.840090	0.937388
2611	−2.789466	0.937928	14491	−2.829761	0.937475	35317	−2.840263	0.937386
2791	−2.791786	0.937898	14911	−2.830177	0.937472	35971	−2.840433	0.937385
2977	−2.793957	0.937870	15337	−2.830581	0.937468	36631	−2.840601	0.937384
3169	−2.795992	0.937844	15769	−2.830974	0.937464	37297	−2.840765	0.937382
3367	−2.797904	0.937820	16207	−2.831356	0.937461	37969	−2.840926	0.937381
3571	−2.799703	0.937798	16651	−2.831728	0.937458	38647	−2.841084	0.937380
3781	−2.801399	0.937777	17101	−2.832090	0.937454	39331	−2.841240	0.937350
3997	−2.803000	0.937758	17557	−2.832442	0.937451	40021	−2.841392	0.937340
4219	−2.804515	0.937740	18019	−2.832786	0.937448	40717	−2.841542	0.937340
4447	−2.805950	0.937723	18487	−2.833120	0.937445	41419	−2.841690	0.937340
4681	−2.807311	0.937707	18961	−2.833446	0.937443	42127	−2.841835	0.937340
4921	−2.808604	0.937692	19441	−2.833763	0.937440	42841	−2.841978	0.937340

Table III. Results ε and a_0 for the 3D cases. We also include the numerical results produced by a more accurate minimization procedure.

3D sphere			3D Lattice			Published numerical results	
N	ε	a_0	N	ε	a_0	N	ε
13	−3.192285	0.986488	8	−1.90962	0.981385	50	−4.89100
57	−3.795009	0.933200	27	−2.87743	0.971893	60	−5.09793
157	−4.479330	0.909165	64	−3.45409	0.966883	70	−5.24131
335	−4.945768	0.898804	125	−3.83547	0.963788	80	−5.35105
615	−5.249568	0.894296	216	−4.10605	0.961686	90	−5.47149
1022	−5.463666	0.892594	343	−4.30787	0.960165	100	−5.57040
1574	−5.626424	0.891092	512	−4.46416	0.959014	100	−5.65262
2298	−5.746206	0.890292	729	−4.58873	0.958111	120	−5.72518
3214	−5.830164	0.890078	1000	−4.69036	0.957385	130	−5.80978
4346	−5.911180	0.889441	1331	−4.77483	0.956788	140	−5.90125
5718	−5.964925	0.889470	1728	−4.84615	0.956289	150	−5.95540
7351	−6.022146	0.889060	2197	−4.90717	0.955865	200	−6.14593
9267	−6.062184	0.888996	2744	−4.95998	0.955500	250	−6.31918
11494	−6.097487	0.888964	3375	−5.00611	0.955184	300	−6.47369
14044	−6.130420	0.888798	4096	−5.04677	0.954906	400	−6.62608
16954	−6.156995	0.888775	4913	−5.08288	0.954660	561	−6.84919
20238	−6.181064	0.888764	5832	−5.11515	0.954441	923	−7.09937
23924	−6.203130	0.888747	6859	−5.14416	0.954245	1415	−7.28543
28026	−6.225377	0.888621	8000	−5.17040	0.954069		
			9261	−5.19423	0.953909		
			10648	−5.21597	0.953763		
			12167	−5.23589	0.953630		
			13824	−5.25421	0.953508		
			15625	−5.27111	0.953395		

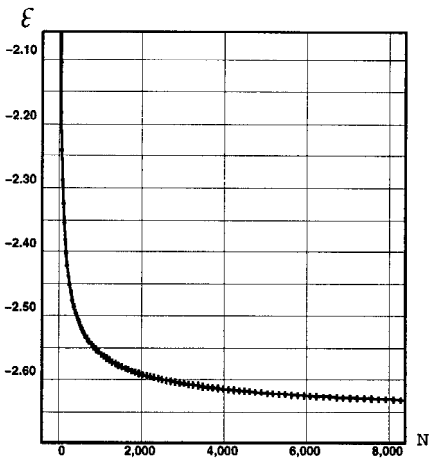

Figure 9. ε versus N for 2D lattice; results (crosses) and fit (line).

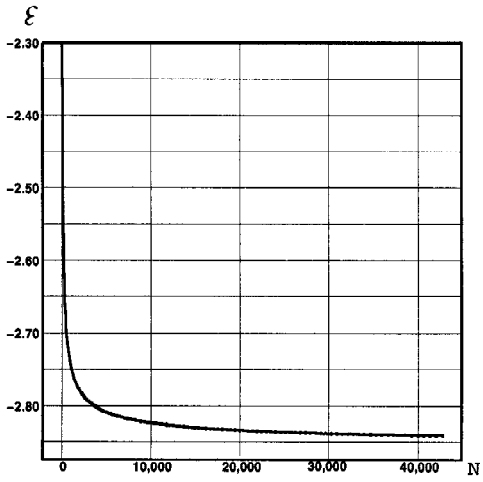

Figure 10. ε versus N for 2D rings; results (crosses) and fit (line).

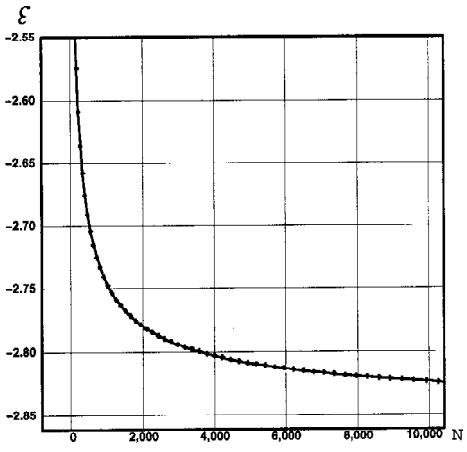

Figure 11. ε versus N for 2D rings; results and fit.

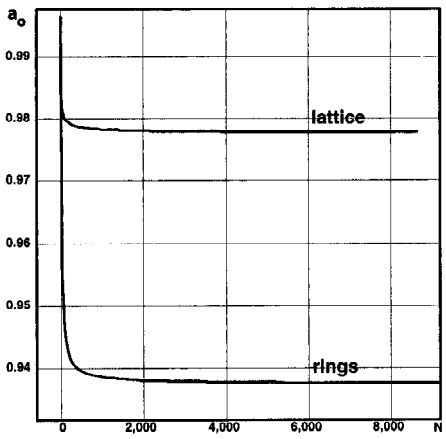

Figure 12. a_0 versus N for 2D lattice and rings.

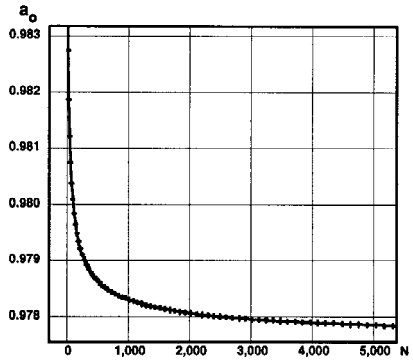

Figure 13. a_0 versus N for 2D lattice; results (crosses) and fit (lines).

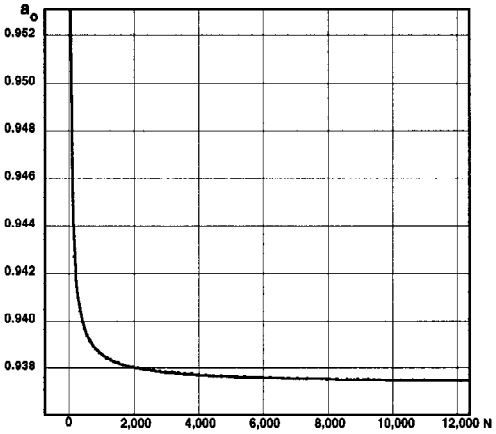

Figure 14. a_0 versus N for 2D rings; results (crosses) and fit (lines).

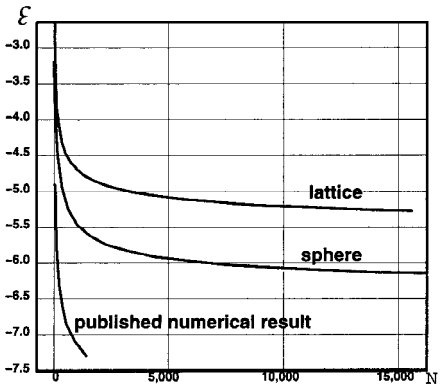

Figure 15. ε versus N for 3D lattice, sphere, and published numerical results.

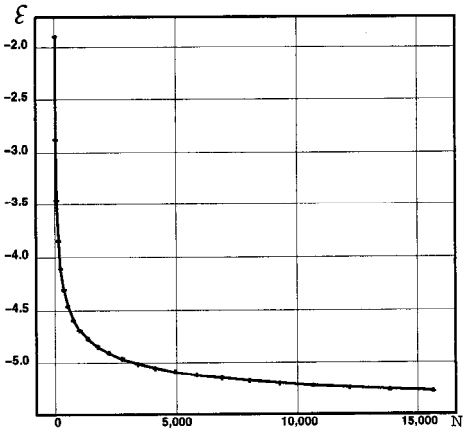

Figure 16. ε versus N for 3D lattice; results (crosses) and fit (line).

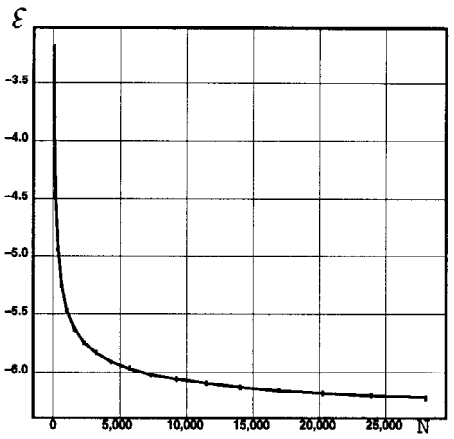

Figure 17. ε versus N for 3D sphere; results (crosses) and fit (line).

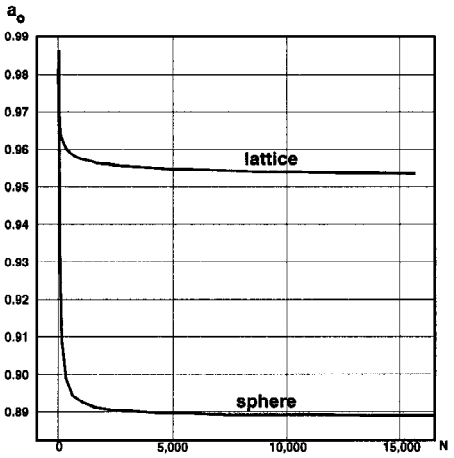

Figure 18. a_0 versus N for 3D lattice and sphere.

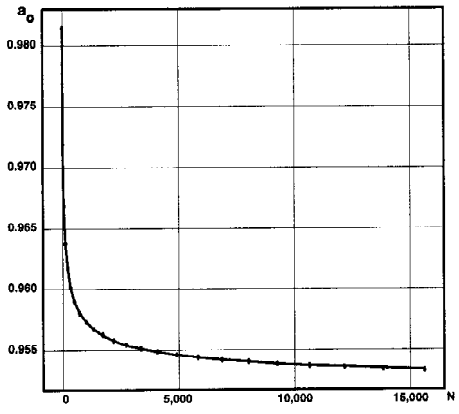

Figure 19. a_0 versus N for 3D lattice; results (crosses) and fit (line).

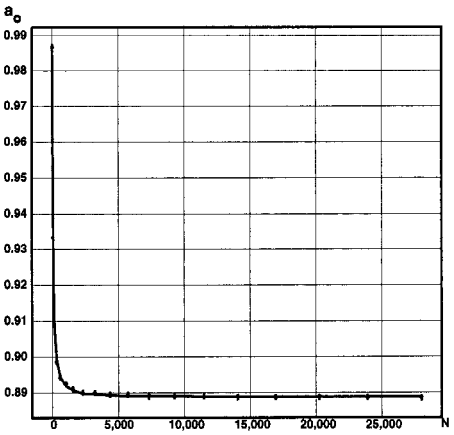

Figure 20. a_0 versus N for 3D sphere; results (crosses) and fit (line).

4. Asymptotic results from the fits

The numerical results look very regular and thus it is tempting to fit them into curves. For the energy, we propose two fitting formulae, ε_I and ε_{II}. We fit the results for the 2D lattice and 2D rings by ε_I and other cases by ε_{II}. The purpose of fitting specific case, by a special formula is to reduce fitting error. In each of these formulae, ε_∞ is the average per-particle energy at $N \to \infty$, while α, β, ε_α, ε_β and ε_N have not found meaningful physical interpretations. For the inter-particle distance, we fit in three different formula, a_I, a_{II} and a_{III}. In each of these formula a_∞ is the asymptotic value at $N \to \infty$ for the average distance. The 2D lattice fits a_I, the 2D rings fit a_{III} and both 3D cases, lattice and sphere, fit a_{II}.

Formulae for ε:
fit ε_I : $\varepsilon(N) = \varepsilon_\infty + \frac{\varepsilon_\alpha}{N^\alpha} + \frac{\varepsilon_\beta}{N^\beta}$
fit ε_{II} : $\varepsilon(N) = \varepsilon_N\, e^{-\alpha N^\beta} + \varepsilon_\infty$
Formulae for a_0:
fit a_I : $a_0(N) = a_\infty + \frac{a_\alpha}{N^\alpha} + \frac{a_\beta}{N^\beta}$
fit a_{II} : $a_0(N) = a_N\, e^{-\alpha N^\beta} + a_\infty$
fit a_{III} : $a_0(N) = a_\infty + a_\alpha\, e^{\alpha N} + \frac{a_\beta}{N^\beta}$

See Tables 4 and 5 for the numerical values of the coefficients as well as for the values of χ^2 indicating the accuracy of our fits.

Table IV. Results for the fittings for E.

ε	fit	χ^2	ε_∞	ε_α	ε_β	ε_N	α	β
2D lattice	ε_I	$3.7{\cdot}10^{-5}$	−2.66592	−2.65475	5.34049		−0.73700	−0.54652
2D rings	ε_I	$5.5{\cdot}10^{-6}$	−2.85726	−10.1903	4.24946		−1.59242	−0.52626
3D lattice	ε_{II}	$1.4{\cdot}10^{-4}$	−5.54535			69.5474	2.48452	0.08270
3D sphere	ε_I	$1.9{\cdot}10^{-4}$	−6.50053	19.5521	−31.5291		−0.41310	−0.86051

Table V. Results for the fittings for a_0.

a_0	fit	χ^2	a_∞	a_α	a_β	a_N	α	β
2D lattice	a_I	$2.7{\cdot}10^{-9}$	0.977509	0.027648	1.82951		−0.516000	−6.561650
2D ring	a_{III}	$8.7{\cdot}10^{-6}$	0.937327	−6.92488	0.35603		−0.888498	−0.081508
3D lattice	a_{II}	$4.3{\cdot}10^{-8}$	0.951598			12.5699	5.45265	0.498000
3D sphere	a_{II}	$2.8{\cdot}10^{-6}$	0.888979			0.692199	1.07462	0.233963

5. Conclusions

We have designed a method to place particles on lattices, spheres and icosahedron to minimize the energy of the Lennard-Jones clusters with very large numbers of particles, approximately, by analytical approaches. Our schemes give the configuration of the clusters only for certain number of particles because of the filling scheme we select. The energies for which our scheme do not give a configuration are calculated by fitting.

Using our methods, we have obtained the asymptotic values for the average per-particle energy and average inter-particle distance. As observed, the spherical scheme produces the most accurate results among the three, which suggests the clusters tend to form spherical structures.

The most significant part of our work is the drastic reduction of parameters for the energy minimization of the Lennard-Jones clusters. Our methods can provide quick initialization for more accurate numerical calculations on small clusters with 1000s of particles. Moreover, our methods can produce estimates for large clusters that no other numerical means can do. Of course, our methods can be further improved by introducing more parameters.

References

1. Leary, R.H. (1997), Global optima of Lennard-Jones clusters, *Journal of Global Optimization* 11: 35–53.
2. Leary, R.H. (1996), A robust gradient descent algorithm for the global optimization of Lennard-Jones clusters. San Diego Supercomputer Center, San Diego, Technical Report GA-A-22514.
3. Northby, J.A. (1987), Structure and binding of Lennard-Jones clusters: $13 \leqslant N \leqslant 147$, *Journal of Chemical Physics* 87: 6166–6178.
4. Pardalos, P.M., Shalloway, D., Xue, G.L. (1994), Optimization methods for computing global minima of non-convex potential energy functions, *Journal of Global Optimization* 4: 117–133.
5. Raoult, B., Farges, J., De Feraudy, M.F., Torchet, G. (1989), Comparison between icosahedral, decahedral, and crystalline Lennard-Jones models containing 500 to 6000 atoms, *Philosophical Magazine* B 60: 881–906.
6. Xie, J., Northby, J.A., Freeman, D.L., Doll, J.D. (1989), Theoretical studies of the energetics and structure of atomic clusters, *Journal of Chemical Physics* 91: 612–619.
7. Xue, G.L. (1994), Improvement of the Northby algorithm for molecular conformation: better solutions, *Journal of Global Optimization* 4: 425–440.
8. Byrd, R.H., Eskow, E., Schnabel, R.B. (1995), A new large-scale global optimization method and its application to Lennard-Jones problems. Technical Report CU-CS-630-92, Department of Computer Science, University of Colorado, revised 1995; also in P.M. Pardalos, D. Shalloway, and G. Xue (eds.), DIMACS Series in Discrete Mathematics and Theoretical Computer Science, Vol. 23, American Mathematical Society, Providence, R.I., 1995.
9. Coleman, T.E., Shalloway, D., Wu, Z. (1994), A parallel build-up algorithm for global energy minimizations of molecular clusters using effective energy simulated annealing, *Journal of Global Optimization* 4: 171–185.
10. Deng, Y., Rivera, C. (1999), Simple energy minimization for huge Lennard-Jones clusters by dramatic parameter reduction, *Appl. Math. Lett.* 12: 119.
11. Pardalos, P.M., Shalloway, D., Xue, G. (1995), Global minimization of nonconvex energy functions: molecular conformation and protein folding. DIMACS workshop, vol. 23.
12. Hargittai, I. (1990), *Quasicrystals, Networks, and Molecules of Fivefold Symmetry.* VCH Publishers.